

Increased Thermoelectric System Thermodynamic Efficiency by Use of Convective Heat Transport

Lon E. Bell

BSST LLC

5462 Irwindale Avenue

Irwindale, CA 91706

lbell@amerigon.com; 626-815-7430

Abstract

The thermodynamic efficiencies of thermoelectric systems are shown to increase in geometries where convective heat transport can be used to effectively reduce internal heat conduction losses within the thermoelectric elements themselves. For the case of one-dimensional, temperature-independent material properties, exact analytic solutions are given. Equations for maximum COP and cooling power are presented, as are equations for maximum COP in heating and maximum efficiency and power output for power generation. Comparisons with standard thermoelectric show efficiency gains of 20% to 50% for important cooling applications. In heating, 40% to 80% gains are shown to be attainable. Power generation benefits and efficiency gains are described. Methods of achieving convective transport are discussed briefly, as are applications to air conditioning, heating and temperature control.

Introduction

Many important thermodynamic systems that use solid-state energy conversion (SSEC) involve at some part of their cycle, convective transport of thermal power. For example, air conditioners, heaters, and heat pumps deliver conditioned air to rooms, production areas, car interiors and the like. Similarly, power generators often extract thermal power from combustion gases, exhaust gases, or moving working fluids such as steam or NaK.

These systems usually are time invariant flow processes, or can be treated as such, because process conditions change slowly compared to the thermal time constants of the system. Quasi-steady-state processes, which lend themselves to comprehensive analysis, govern their performance. The use of working fluids in conjunction with SSEC systems to improve system efficiency has not received significant attention. A time-varying cycle was explored by Echigo, et al. ⁽¹⁾ at the time this author first explored and derived the basic equations presented in this paper. Each work started at about the same time, but was done independently. This work was further developed by Tada, et al. ^(2,3) and was investigated and results published over the ensuing years. Work on the subject by this author continued up to the present but has not been published previously.

The premise of the present work is that by the incorporation of convective heat flow into the thermodynamic cycle, the thermodynamic efficiency of a quasi-steady-state SSEC system utilizing thermoelectric or thermionic effects, the thermodynamic efficiency can be improved beyond that for such systems operating in a standard manner. In the first section of this paper, the basic

concepts are presented and the standard equations for thermoelectric systems are described in a form useful to the analyses of the new system. In the next section, the operation of systems employing convection is discussed, and the underlying equations are compared to those of the standard geometry.

Equations are developed the third section for three distinct cases of interest: heating, cooling and power generation. Equations for maximum and most efficient energy conversion are derived. Examples of applications for each case are given along with a brief discussion of system characteristics. Limitations and positive attributes are noted. Section Four presents a summary and conclusions.

For conceptual purposes, this analysis is carried out assuming the thermoelectric materials are liquids. However, the analysis is directly applicable to moving solid TE materials, and is readily modified to describe flow of a working fluid through porous TE material. In two-phase systems, the thermal conductance, K , must be modified to include a contribution from the conductivity of the convective fluid, and for more representative simulations, local temperature non-equilibrium between the fluid and the TE material must be added to the model. For air, most other gases and typical organic liquids, the effect of conductance is quite small, but the impact of non-equilibrium can be more significant.

1.0 Analysis

To introduce the basic concepts of this paper, consider a thermoelectric couple in which both the N and P thermoelectric elements are liquid materials. Assume that electrical resistivity, thermal conductivity and Seebeck coefficient are temperature independent. Further, assume the containment members for the thermoelectric liquids have negligible effect on the system and can be ignored. Finally, assume time-independent one-dimensional flow. The system described is shown schematically in Figure 1. Each fluid has properties designated by the subscript N or P to identify the two separate legs of a thermoelectric couple. The direction of electron flow is in a generally counter-clockwise direction. With electrical power applied, T_{OUT} will be the hotter side and T_{IN} the colder.

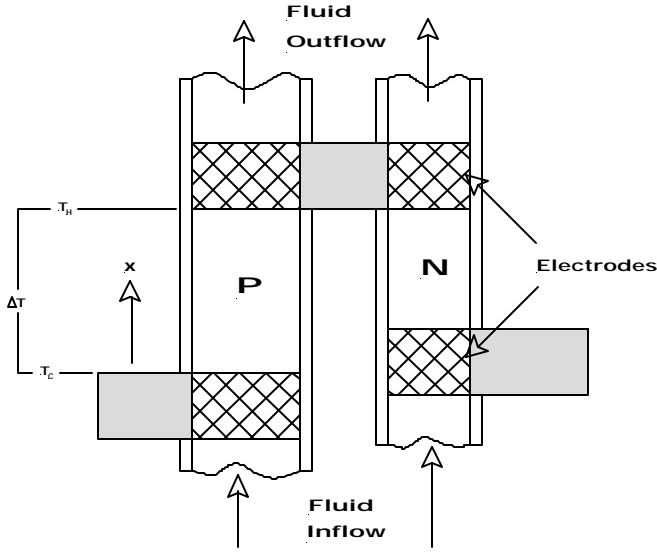


Figure 1.

For the moment, assume there is no fluid movement and the thermal conductivities of the fluid external to the couple can be ignored. In this case, the equations for the conventional system, following Angrist⁽⁴⁾, can be developed from the basic heat flow equation for each leg of the thermoelectric couple;

$$(1) \mathbf{I}_N T_N''(x) + J_N^2 \mathbf{r}_N = 0$$

and;

$$(2) \mathbf{I}_P T_P''(x) + J_P^2 \mathbf{r}_P = 0$$

where, for the leg under consideration

$\mathbf{I}_{N,P}$ = material thermal conductivity

$\mathbf{r}_{N,P}$ = material electrical conductivity

$J_{N,P}$ = current density

$T_{N,P}(x)$ = temperature as a function of x

Using the same boundary conditions for each leg,

$$(3) T_{N,P}(0) = T_C$$

$$T_{N,P}(x) = T_H$$

$$(4) \Delta T = T_H - T_C$$

$T_{N,P}(x)$ is found to be;

$$(5) T_{N,P}(x) = T_C + \Delta T \frac{x}{l_{N,P}} + \frac{J_{N,P}^2 \mathbf{r}_{N,P} l_{N,P}}{2 \mathbf{I}_{N,P}} x \left(1 - \frac{x}{l_{N,P}}\right)$$

Performance is optimized for the two legs if they satisfy;

$$(6) RK = \left[(\mathbf{r}_N \mathbf{I}_N)^{\frac{1}{2}} + (\mathbf{r}_P \mathbf{I}_P)^{\frac{1}{2}} \right]^2$$

where;

$$(7) R = \frac{\mathbf{r}_N l_N}{a_N} + \frac{\mathbf{r}_P l_P}{a_P}$$

$$(8) K = \frac{\mathbf{I}_N a_N}{l_N} + \frac{\mathbf{I}_P a_P}{l_P}$$

and;

$a_{N,P}$ = cross-sectional area of leg (N, P)

$l_{N,P}$ = length of leg (N, P)

Let;

$$(9) \mathbf{a} = (\mathbf{a}_P - \mathbf{a}_N)$$

Where;

$a_{N,P}$ = Seebeck coefficient of leg (N,P)

Further, let;

$$(10) I = J_{N,P} a_{N,P}$$

Under these conditions, the temperature profile in each leg is similar and;

$$(11) T(x) = T(0) + \frac{\Delta T}{2} \frac{x}{l} + \frac{I^2 R}{2K} \frac{x}{l} \left(1 - \frac{x}{l}\right)$$

and the heat transport Equations (1) and (2) become this single equation.;

$$(12) 0 = KT''(x) + \frac{I^2 R}{l^2}$$

In the following parts, parameters for the P-type and N-type legs will be lumped into a single equation similar to Equation (12). Obviously, a single leg could have convective transport. In this case, the equations would be applied to that leg, and the equation developed above would apply to the other leg.

2.0 Heating

Figure 2 is a schematic that combines the individual TE elements into a single one-dimensional system suitable for the analyses that follow.

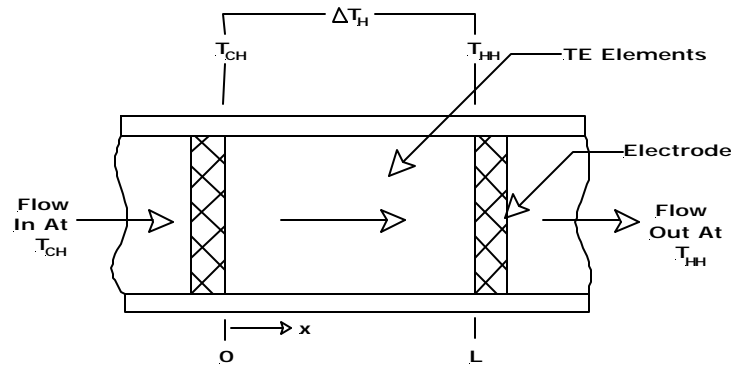


Figure 2.

The thermal power in heating, q_H , is the Peltier term, $\mathbf{a}IT_{HH}$, plus the net conductive heat flux out the hot side;

$$(13) q_H = \mathbf{a}IT_{HH} + I^2 R - Kl \frac{dT_H(0)}{dx}$$

which, when used in Equation (11) becomes the familiar;

$$(14) q_H = \mathbf{a}IT_{HH} + \frac{1}{2} I^2 R - K \Delta T_H$$

where the subscript H denotes heating. Consider the

equivalent derivations for the complete system in Figure 2. Including convection, for which it is assumed the liquid TE materials in Figure 2 are one-dimensional and move in the x direction (from the cold to hot side);

$$(15) 0 = \mathbf{I}_N T''(x) - C_{PN} m_N T'(x) + J_N^2 \mathbf{r}_N$$

$$(16) 0 = \mathbf{I}_P T''(x) - C_{PP} m_P T'(x) + J_P^2 \mathbf{r}_P$$

where, for each leg;

$C_{N,P}$ = heat capacity per unit mass of the (N, P) material

$m_{N,P}$ = mass flow rate per unit area of the (N, P) material

With the same optimization as in Equation (6), Equations (15) and (16) can be written as a single heat flow equation;

$$(17) 0 = K T_H''(x) - \frac{C_P m}{l} T_H'(x) + \frac{I^2 R}{l^2}$$

where;

$$(18) C_P m = C_{PN} m_N a_N + C_{PP} m_P a_P$$

It is useful to define a parameter \mathbf{d} as the ratio of convective heat transport to conductive heat transport;

$$(19) \mathbf{d}_H = \frac{C_P m}{K}$$

$$(20) 0 = T_H''(x) - \frac{\mathbf{d}_H}{l} T_H'(x) + \frac{I^2 R}{K l^2}$$

With the same boundary conditions as in Equation (3), the solution to Equation (20) is;

$$(21) T_H(x) = T_H(0) + \frac{I^2 R}{\mathbf{d}_H K} \frac{x}{l} + \left(\Delta T_H - \frac{I^2 R}{\mathbf{d}_H K} \right) \left(\frac{e^{\frac{\mathbf{d}_H x}{l}} - 1}{e^{\mathbf{d}_H} - 1} \right)$$

The convective plus conductive heat flux out the hot side, q_H^* , is;

$$(22) q_H^* = \mathbf{a} I T_{HH} + I^2 R - K l \frac{dT(0)}{dx}$$

Equation (22) is the equivalent to Equation (13), with $T_H(l) = T_{HH}$

At $x=0$, the incoming convective thermal heat flux is zero if the fluid enters at temperature $T_H(0)$

then;

$$(23) q_H^* = \mathbf{a} I T_{HH} + \frac{\mathbf{x}(\mathbf{d}_H)}{2} I^2 R - \mathbf{z}(\mathbf{d}_H) K \Delta T_H$$

where;

$$(24) \mathbf{x}(\mathbf{d}) = \frac{2}{\mathbf{d}} \left(\frac{\mathbf{d} e^{\mathbf{d}} - e^{\mathbf{d}} + 1}{e^{\mathbf{d}} - 1} \right)$$

$$(25) \mathbf{z}(\mathbf{d}) = \frac{\mathbf{d}}{e^{\mathbf{d}} - 1}$$

Notice that if $\mathbf{d} \rightarrow 0$, $\mathbf{x}(0) \rightarrow 1$ and $\mathbf{z}(0) \rightarrow 1$ corresponding to the case without convection,

that is, Equation (14). The new parameter $\mathbf{x}(\mathbf{d})$ is the portion of the Joule heating swept to the hot side by convection, and $\mathbf{z}(\mathbf{d})$ is the portion of conductive losses lost to the cold side with convection.

Figure 3 presents $\mathbf{x}(\mathbf{d})$ and $\mathbf{z}(\mathbf{d})$ as a function of \mathbf{d} .

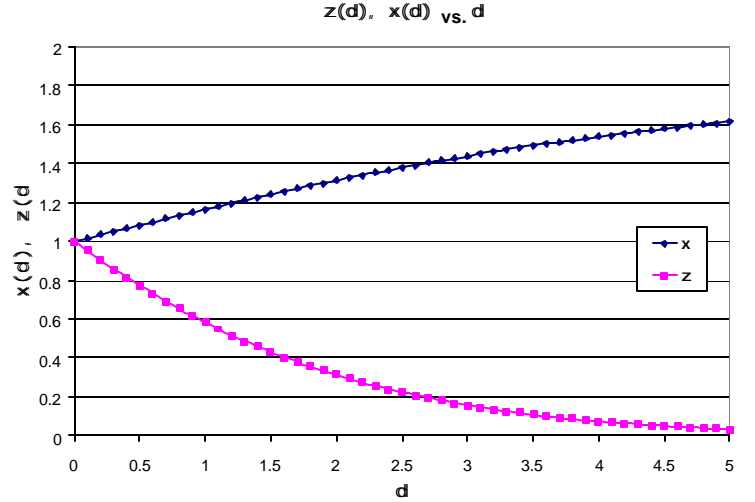


Figure 3.

The condition where the convective heat flux exactly equals q_H^* is of special interest, as it defines the practical maximum value for \mathbf{d}_H in heating. Calling this value \mathbf{d}_{HM} ;

$$(26) q_H^* = C_P m \Delta T_H = \mathbf{d}_{HM} K \Delta T_H$$

Equating Equation (26) to Equation (23) yields;

$$(27) (\mathbf{z}(\mathbf{d}_{HM}) + \mathbf{d}_{HM}) K \Delta T_H = \mathbf{a} I T_{HH} + \frac{\mathbf{x}(\mathbf{d}_{HM}) I^2 R}{2}$$

Equations (14), (23) and (27) can be recast in terms of Z and ϵ , where;

$$(28) Z = \frac{\mathbf{a}^2}{R K}$$

$$(29) \epsilon = \frac{I R}{\mathbf{a} T_{HH}}$$

The results are;

$$(30) q_H = K Z T_{HH}^2 \epsilon \left(1 + \frac{\epsilon}{2} - \frac{\Delta T_H}{Z T_H^2 \epsilon} \right)$$

$$(31) q_H^* = K Z T_{HH}^2 \epsilon \left(1 + \frac{\epsilon \mathbf{x}(\mathbf{d}_{HM})}{2} - \frac{\mathbf{z}(\mathbf{d}_{HM}) \Delta T_H}{Z T_H^2 \epsilon} \right)$$

$$(32) (\mathbf{z}(\mathbf{d}_{HM}) + \mathbf{d}_{HM}) \Delta T_H = Z T_{HH}^2 \epsilon \left(1 + \frac{\epsilon \mathbf{x}(\mathbf{d}_{HM})}{2} \right)$$

Equation (32) can be rewritten as a function of ϵ and \mathbf{d}_{HM} ;

$$(33) \frac{\Delta T_H}{ZT_{HH}^2} = \epsilon \frac{\left(1 + \frac{x(d_{HM})}{2}\right)}{\left(z(d_{HM}) + d_{HM}\right)}$$

The right side is independent of Z.

$T_H(x)/T_{HH}$ vs. x/l
for $\nu = .5$ and $ZT_{HH} = 1$

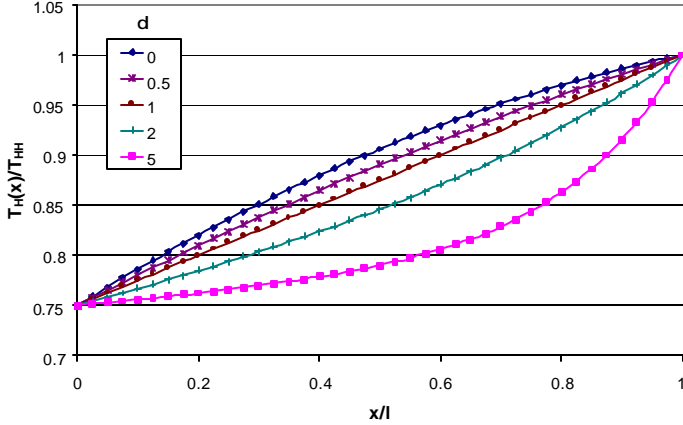


Figure 4.

Figure 4 presents typical temperature profiles for conduction, ($d_H = 0$), and various amounts of convection. As d_H increases, the profile changes from the traditional parabolic profile to ones affected by convection. The slope at $x=0$ is reduced by convection, indicating heat loss to the cold side is less.

d_{HM} vs. $\Delta T_H/T_{HH}$
For $ZT_{HH} = 1$

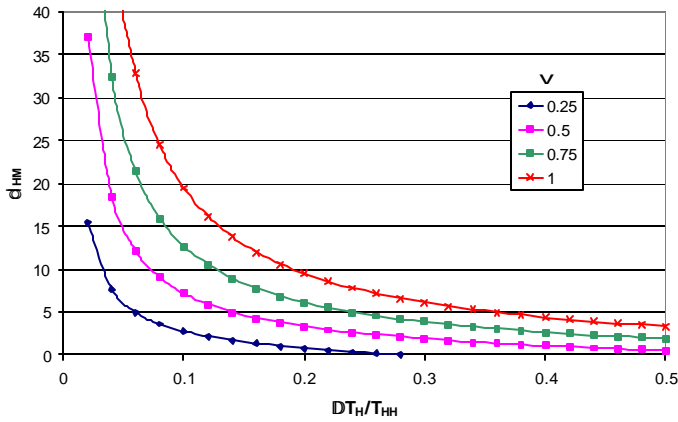


Figure 5.

Figure 5 gives the relationship between d_{HM} and $\Delta T_H/T_{HH}$ for $ZT_{HH} = 1$ and several values of ϵ . Figure 6 gives d_{HM} as a function $\Delta T_H/T_{HH}$ for $\epsilon = .5$ and several values of ZT_{HH} .

d_{HM} vs. $\Delta T_H/T_{HH}$
For $\nu = .5$

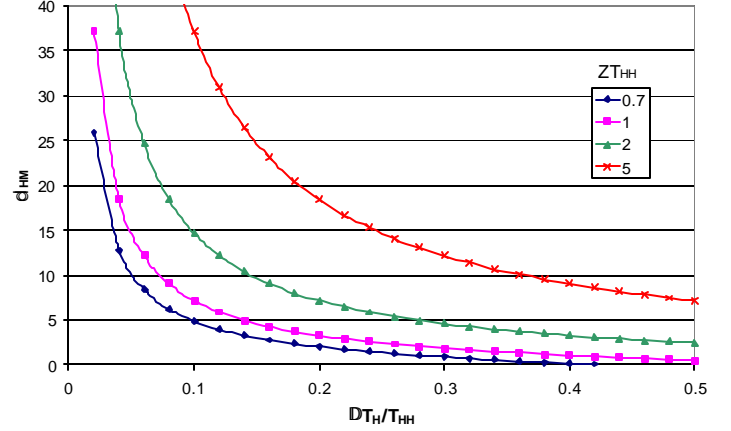


Figure 6.

The power supplied to the system, q_{IN} , is the voltage times the current, that is, IV , where the voltage has two components; one from the Seebeck voltage at the junctions and the other from the normal Joule loss. Thus;

$$(34) V = a \Delta T + IR$$

$$(35) q_{IN} = IV = a I \Delta T_H + I^2 R$$

In terms of ZT_{HH} and ϵ , Equation (35) can be written using Equations (28) and (29) as;

$$(36) q_{IN} = KZT_{HH}^2 \epsilon \left[\frac{\Delta T_H}{T_{HH}} + \epsilon \right]$$

The coefficients of performance (COP) in heating for conduction, f_H and convection, g_H , are the ratios of q_H and q_H^* to the input power, q_{IN} , from Equation (36). From Equations (30), (31) and (36), the COPs are;

$$(37) f_H = \frac{1 + \frac{\epsilon}{2} - \frac{\Delta T_H}{ZT_{HH}^2} \epsilon}{\frac{\Delta T_H}{T_{HH}} + \epsilon}$$

$$(38) g_H = \frac{1 + \frac{\epsilon x(d_H)}{2} - \frac{z(d_H) \Delta T_H}{ZT_{HH}^2} \epsilon}{\frac{\Delta T_H}{T_{HH}} + \epsilon}$$

The ratio of performance of the two is;

$$(39) \frac{g_H}{f_H} = \frac{1 + \frac{\epsilon x(d_H)}{2} - \frac{z(d_H) \Delta T_H}{ZT_{HH}^2} \epsilon}{1 + \frac{\epsilon}{2} - \frac{\Delta T_H}{ZT_{HH}^2} \epsilon}$$

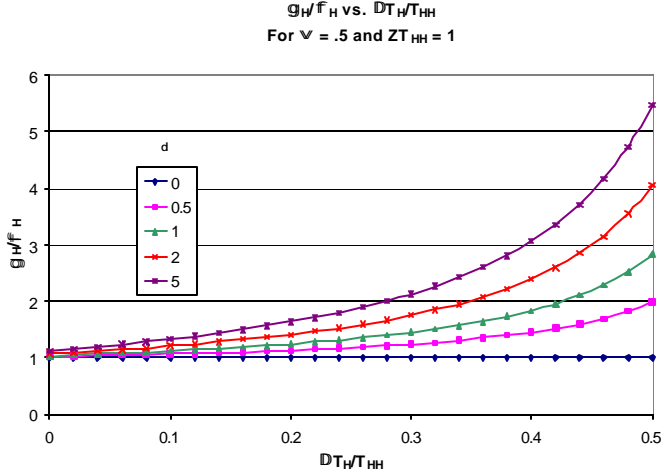


Figure 7.

Figure 7 is a plot of the ratio of convective COP , g_H to conductive COP , f_H as a function of $\Delta T_H/T_{HH}$ for $ZT_{HH} = 1$, $\epsilon = .5$ and several values of d . Figure 8 presents the same ratio for various values of ϵ , $ZT_{HH} = 1$ and against d . In the figure, curves are terminated at d_{CM} .

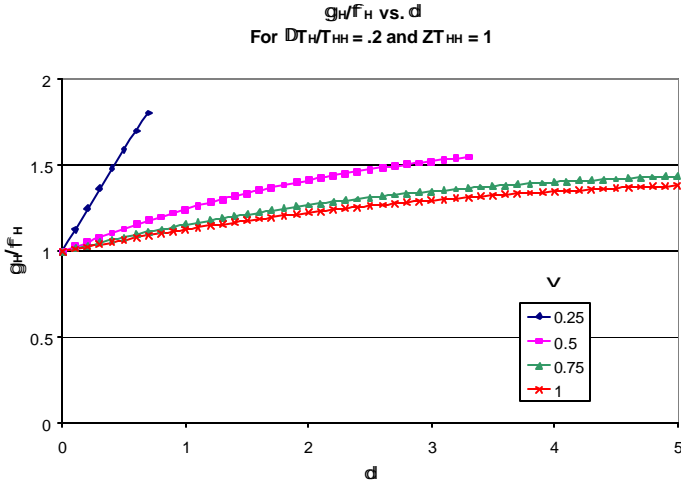


Figure 8.

3.0 Cooling

The same energy balance Equations, (12) and (17), can be used to develop cooling equations that correspond to the heating equations treated above. The cooling power in conventional conductive systems, q_C , is given by

subtracting the heat conducted in at the hot end plus Joule heating generated throughout the system from the Peltier cooling at the cold end;

$$(40) \quad q_C = \mathbf{a} I T_C(0) - I^2 R - Kl \frac{dT_C(l)}{dx}$$

The temperature $T(x)$ is given in Equation (11). Substitution yields the well-known expression;

$$(41) \quad q_C = \mathbf{a} I T_{CC} - \frac{1}{2} I^2 R - K \Delta T_C$$

where;

$$(42) \quad T_{CC} = T_C(0)$$

$$(43) \quad \Delta T_C = T_C(l) - T_C(0)$$

Similarly, the convective cooling power, q_C^* ;

$$(44) \quad q_C^* = \mathbf{a} I T_C(0) - I^2 R - Kl \frac{dT_C(l)}{dx}$$

Where here $T_C(x)$ is the same as $T_H(x)$ in Equation (21).

In cooling, for optimum performance, the convective medium enters from the hot (ambient) side, so it is convenient to make the sign of d_C for cooling negative;

$$(45) \quad d_C = -\frac{C_p m_C}{K}$$

since the conductive heat flux $K \Delta T_C$, and the flux due to the convected medium have the opposite signs. It is assumed that the convected medium enters at temperature T_{HC} , where;

$$(46) \quad T_C(l) = T_{HC}, T_C(0) = T_{CC}$$

$$(47) \quad \Delta T_C = T_C(l) - T_C(0) = T_{HC} - T_{CC}$$

and Equation (20) with the sign convention for d_C changed becomes;

$$(48) \quad 0 = T_C''(x) + \frac{d_C}{l} T_C'(x) + \frac{I^2 R}{Kl^2}$$

which has the solution;

$$(49) \quad T_C(x) = T_{CC} - \frac{I^2 R}{d_C K} \frac{x}{l} + \left(\Delta T_C + \frac{I^2 R}{d_C K} \right) \left(\frac{1 - e^{-d_C \frac{x}{l}}}{1 - e^{-d_C}} \right)$$

Figure 9 presents temperature profiles for $T_C(x)$ for several values of d_C convection steepens the profile at $x = 0$ and reduces conductive loss at $x = l$.

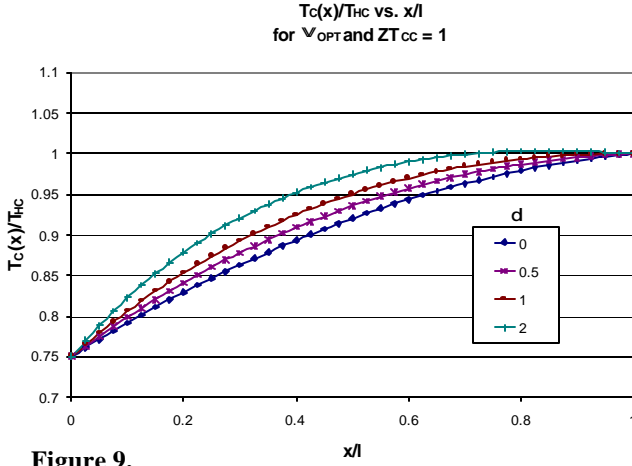


Figure 9.

Note that q_c from Equation (44) can be written using Equation (48) for the derivative of the temperature as;

$$(50) \quad q_c = \mathbf{a} I T_{CC} - \frac{\mathbf{x}(\mathbf{d}_c)}{2} I^2 R - \mathbf{z}(\mathbf{d}_c) K \Delta T_c$$

where the functions $\mathbf{x}(\mathbf{d})$ and $\mathbf{z}(\mathbf{d})$ are defined by Equations (24) and (25). The power into the system for either the conductive or the convective case remains the same as that for heating, given in Equation (36).

The $COPs$ for conduction, \mathbf{f}_c , and convection, \mathbf{b}_c , are defined as;

$$(51) \quad \mathbf{f}_c = \frac{q_c}{q_{IN}}$$

$$(52) \quad \mathbf{b}_c = \frac{q_c^*}{q_{IN}}$$

In terms of ϵ , Z and $T_c(0) = T_{CC}$ and Equations (36), (41) and (50); Equations (51) and (52) can be written as;

$$(53) \quad \mathbf{f}_c = \frac{1 - \frac{\epsilon}{2} - \frac{\Delta T_c}{Z T_{CC}^2} \epsilon}{\frac{\Delta T_c}{T_{CC}} + \epsilon}$$

$$(54) \quad \mathbf{b}_c = \frac{1 - \frac{\mathbf{x}(\mathbf{d}_c)}{2} \epsilon - \frac{\mathbf{z}(\mathbf{d}_c) \Delta T_c}{Z T_{CC}^2} \epsilon}{\frac{\Delta T_c}{T_{CC}} + \epsilon}$$

where here;

$$(55) \quad \epsilon = \frac{I R}{\mathbf{a} T_{CC}}$$

The ratio of \mathbf{b}_c to \mathbf{f}_c is;

$$(56) \quad \frac{\mathbf{b}_c}{\mathbf{f}_c} = \frac{1 - \frac{\mathbf{x}(\mathbf{d}_c)}{2} \epsilon - \frac{\mathbf{z}(\mathbf{d}_c) \Delta T_c}{Z T_{CC}^2} \epsilon}{1 - \frac{\epsilon}{2} - \frac{\Delta T_c}{Z T_{CC}^2} \epsilon}$$

Before discussing the results from Equation (54), it

is important to recognize the limitation to the magnitude of \mathbf{d}_c imposed by the maximum available heat flux, q_c . Analogous to heating, \mathbf{d}_c reaches a practical maximum when all of the cooling power is transferred to the convective medium that is;

$$(57) \quad q_c^* = -C_p m \Delta T_c = \mathbf{d}_c K \Delta T_c$$

$$(58) \quad = \mathbf{a} I T_{CC} - \frac{\mathbf{x}(\mathbf{d}_c)}{2} I^2 R - \mathbf{z}(\mathbf{d}_{CM}) K \Delta T_c$$

Thus, \mathbf{d}_{CM} , the effective maximum value of \mathbf{d}_c is found by equating Equations (57) and (58);

$$(59) \quad (\mathbf{d}_{CM} + \mathbf{z}(\mathbf{d}_{CM})) K \Delta T_c = \mathbf{a} I T_{CC} - \frac{\mathbf{x}(\mathbf{d}_{CM})}{2} I^2 R$$

And in terms of ϵ and $Z T_{CC}$;

$$(60) \quad \frac{\Delta T_c}{T_{CC}} = Z T_{CC} \epsilon \left(\frac{1 - \frac{\epsilon \mathbf{x}(\mathbf{d}_{CM})}{2}}{\mathbf{z}(\mathbf{d}_{CM}) + \mathbf{d}_{CM}} \right)$$

The maximum temperature differential, ΔT_{CMAX} is found by determining the value of I that maximizes q_c in Equation (41), and then setting $q_c = 0$ and solving for ΔT_{CMAX} . The result, in terms of Z is;

$$(61) \quad \frac{\Delta T_{CMAX}}{T_{CC}} = \frac{Z T_{CC}}{2}$$

which is well known.

Combining Equations (60) and (61), the relationship for \mathbf{d}_{CM} can be given in terms of $\Delta T_c / \Delta T_{CMAX}$ and ϵ . The result is independent of Z ;

$$(62) \quad \frac{\Delta T_c}{\Delta T_{CMAX}} = 2 \epsilon \left(\frac{1 - \frac{\epsilon \mathbf{x}(\mathbf{d}_{CM})}{2}}{\mathbf{z}(\mathbf{d}_{CM}) + \mathbf{d}_{CM}} \right)$$

The optimum dimensionless current ϵ_{OD} for the conduction case is found by differentiating \mathbf{f}_c in Equation (53) with respect to ϵ , and setting the result to zero. The familiar result for ϵ_{OD} is;

$$(63) \quad \epsilon_{OD} = \frac{\Delta T_c}{T_{CC}} \left(\frac{1}{\sqrt{1 + Z T_{AVE}} - 1} \right)$$

which can be written as;

$$(64) \quad \epsilon_{OD} = \frac{\Delta T_c}{T_{CC}} \frac{1}{M_c - 1}$$

where;

$$(65) \quad M_c = \sqrt{1 + Z T_{AVE}}$$

$$(66) T_{AVE} = \frac{T_{CH} + T_{CC}}{2}$$

If this value is used in Equation (53), the optimum COP , \mathbf{f}_{CO} , is found to be the well-known result;

$$(67) \mathbf{f}_{CO} = \frac{T_{CC}}{\Delta T_C} \left(\frac{M_C - 1 - \frac{\Delta T_C}{T_{CC}}}{M_C + 1} \right)$$

Similarly, the optimum dimensionless current ϵ_{OV} for convection is found from Equation (54). It can be seen from Figure 3 that the functional form of $\mathbf{x}(\mathbf{d})$ and $\mathbf{z}(\mathbf{d})$ are such that as \mathbf{d} increases, $\mathbf{z}(\mathbf{d})$ decreases more rapidly than $\mathbf{x}(\mathbf{d})$ increases. Thus, the effect of increasing \mathbf{d} reduces proportionally the losses due to the conductive heating more than it increases the convective contribution from Joule heating. Both terms are about equal if for $\mathbf{d} = 0$. The magnitude of the conduction term is larger for large ΔT or small ϵ . Thus, for certain values of ΔT_C , ϵ and \mathbf{d}_C , there can be a net gain in system efficiency (COP) with convection. The expression for the optimum dimensionless current, ϵ_{OV} for convection is found by the same process as that for ϵ_{OD} . The result is;

$$(68) \epsilon_{OV} = \frac{\Delta T_C}{T_{CC}} \left(\frac{1}{M_C(\mathbf{d}_C) - 1} \right)$$

where;

$$(69) M_C(\mathbf{d}_C) = \sqrt{1 + \frac{ZT_{AVE}d}{\mathbf{z}(\mathbf{d}_C)}}$$

and;

$$(70) T_{AVEd} = T_{CC} + \frac{\mathbf{x}(\mathbf{d}_C)}{2} \Delta T_C$$

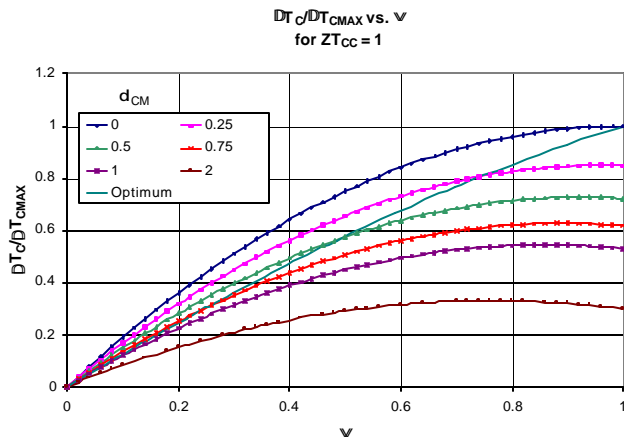


Figure 10.

Figure 10 shows the relationship between

$\Delta T_C / \Delta T_{C_{MAX}}$ and ϵ for the several values of \mathbf{d}_C . The solid line plotted in Figure 10 gives the relationship between $\Delta T_C / \Delta T_{C_{MAX}}$ and the optimum ϵ , ϵ_{OV} . Unlike the other curves in Figure 10, ϵ_{OV} is dependent on Z . Here, results are given for $ZT_{CC} = 1$.

The optimum COP , \mathbf{b}_{CO} , is found by using Equation (68) in Equation (54);

$$(71) \mathbf{b}_{CO} = \frac{T_{CC}}{\Delta T_C} \left(\frac{M_C(\mathbf{d}_{CO}) - 1 - \frac{\mathbf{x}(\mathbf{d}_{CO}) \Delta T_C}{T_{CC}}}{M_C(\mathbf{d}_{CO}) + 1} \right)$$

It can be seen from Equation (71) that \mathbf{b}_{CO} can benefit from convection, since from Equation (69), $M_C(\mathbf{d}_C)$ can be larger than M_C because of two factors. First, the term $Z/\mathbf{z}(\mathbf{d}_C)$ effectively increases Z by the inverse of $\mathbf{z}(\mathbf{d}_C)$. Thus, the figure of merit $Z = \mathbf{a}^2 / KR$ is increased by the apparent reduction in the thermal conductance K . The average temperature T_{AVEd} also increases but by a lesser amount (it is often negligible). The last term in the numerator in Equation (71) has the opposite effect and reduces COP in proportion to the magnitude of $\mathbf{x}(\mathbf{d}_C)$. Nevertheless, for many operating regimes of interest, the gain in $M_C(\mathbf{d}_C)$ outweighs the reduction from $\mathbf{x}(\mathbf{d}_C)$.

Figure 11 gives the ratio $\mathbf{b}_C / \mathbf{f}_C$ as a function of \mathbf{d}_C for several values of ϵ with $ZT_{AVE} = 1$ and $\Delta T_C / \Delta T_{C_{MAX}} = 0.2$. In the Figure, the curves are terminated at \mathbf{d}_{CM} . Figure 12 shows the value of $\mathbf{b}_C / \mathbf{f}_C$ as a function of \mathbf{d}_C for several values of ZT_{CC} . Again, the curves terminate at \mathbf{d}_{CM} .

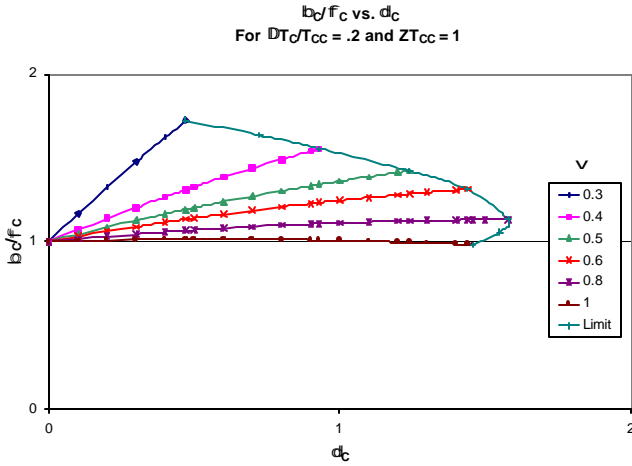


Figure 11.

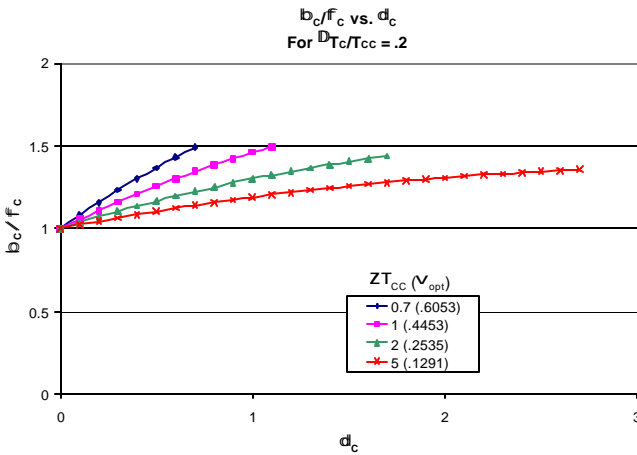


Figure 12.

4.0 Power Generation

Thermoelectric systems can be operated to convert heat flow to electrical power. The basics equation for heat flow is Equation (17), the same as for heating. Here, the subscript P will be used to denote power generation. Equations, unless noted otherwise, will be the same as those for heating.

The derivation of the basic equations for power generation are quite similar to those for heating except a heat source at temperature $T_p(l) = T_{HP}$ and a heat sink at temperature $T_p(0) = T_{CP}$ create a heat flux from l to 0 in the absence of an applied voltage. The thermal flux entering from the hot side (heat source) and that portion exiting the cold side (heat sink) create Seebeck voltages V_p at each end with the sum equal to;

$$(72) V_p = \mathbf{a} \Delta T_p = IR$$

where;

$$(73) \Delta T_p = T_p(l) - T_p(0)$$

$$(74) = T_{HP} - T_{CP}$$

The general arrangement is shown in Figure 13.

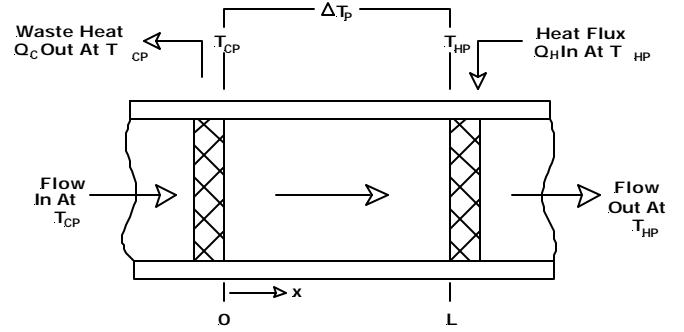


Figure 13.

The net electrical power produced goes to an external load R_l . The work output W_l is;

$$(75) W_l = I^2 R_l$$

The induced current I , creates Joule heating as in the previous cases. For conduction, the temperature $T(x)$ within the system satisfies Equation (11).

Heat flux q_p entering the hot side at l is the heat absorbed by the Peltier junction at l , $\mathbf{a} I T_{HP}$, plus the heat flux into the system at l ;

$$(76) q_p = \mathbf{a} I T_{HP} + Kl \frac{dT_p(l)}{dx}$$

Using $T(x)$ from Equation (11) yields;

$$(77) q_p = \mathbf{a} I T_{HP} - \frac{1}{2} I^2 R + K \Delta T_p$$

Here, R is the internal resistance and is defined as;

$$(78) R_i = \frac{\mathbf{r}_p l_p}{A_p} + \frac{\mathbf{r}_n l_n}{A_n}$$

and the definitions of K , Z and x remain unchanged. The internal plus external load resistances are the total resistance R_t ;

$$(79) R_t = R_i + R_l$$

The current I is the Peltier voltage from Equation (72) divided by the system resistance;

$$(80) I = \frac{\mathbf{a} \Delta T_p}{R_i + R_l}$$

The power produced is;

$$(81) W_l = I^2 R_l$$

and the resultant system efficiency \mathbf{f}_p is;

$$(82) \mathbf{f}_p = \frac{W_l}{q_p}$$

or in terms of Equations (77) and (81), the familiar result is;

$$(83) \mathbf{f}_p = \frac{I^2 R_l}{\mathbf{a} I T_{HP} - \frac{1}{2} I^2 R_i + K \Delta T_p}$$

The optimum efficiency is found by introducing a new variable M_p , where;

$$(84) M_p = \frac{R_i}{R_i}$$

so that Equation (83), written in terms of M_p and Z becomes;

$$(85) \mathbf{f}_p = \frac{\Delta T_p}{T_{HP}} \left(\frac{M_p}{M_p + 1 - \frac{\Delta T_p}{2T_{HP}} + \frac{(M_p + 1)^2}{ZT_{HP}}} \right)$$

The derivative of \mathbf{f}_p with respect to M_p , can be set equal to zero to yield the optimum value of the resistance ratio M_{p0} ;

$$(86) M_{p0} = \sqrt{1 + ZT_{AVE}}$$

where;

$$(87) T_{AVE} = \frac{T_p(l) + T_p(0)}{2} = \frac{T_{HP} + T_{CP}}{2}$$

Substituting Equation (86) into Equation (85) yields another familiar result;

$$(88) \mathbf{f}_{p0} = \frac{\Delta T_p}{T_{HP}} \left(\frac{1}{1 + \frac{2(M_{p0} + 1)}{ZT_{HP}}} \right)$$

For convection with fluid entering at $T_p(0)$ and flowing from the cold side ($x = 0$) to the hot end ($x = l$), the heat flux into the system becomes;

$$(89) q_p = \mathbf{a} IT_{HP} + Kl \frac{dT_p(l)}{dx} - C_p m \Delta T_p$$

The last term, the convective heat flux, must be addressed with care as it is contained in a solid TE material or a working fluid passing through porous thermoelectric materials, etc. Further, it can contain a substantial fraction of the system's thermal power. However, the thermal power contained in the media has to be extracted in an efficient, useful form, or it must be derated or excluded from efficiency calculations. This matter will be addressed in detail at the end of this section. For this analysis, the thermal flux contained in this term will be identified and treated in two sets of equations.

The temperature profile for power generation can be found from Equation (21) with subscript H replaced by p to designate power and R replaced by R_i , the system's internal resistance;

$$(90) T_p(x) = T_p(0) + \frac{I^2 R_i x}{d_p K l} + \left(\Delta T_p - \frac{I^2 R_i}{d_p K} \right) \left(\frac{e^{d_p \frac{x}{l}} - 1}{e^{d_p} - 1} \right)$$

substituting Equation (90) into Equation (89) yields;

$$(91) q_{pv}^*(\mathbf{d}_p) = \mathbf{a} IT_{HP} + \mathbf{z}(\mathbf{d}_p) K \Delta T_p - \frac{\mathbf{x}(\mathbf{d}_p)}{2} I^2 R_i + \mathbf{d}_p K \Delta T_p$$

For $q_{pv}^*(\mathbf{d}_c)$ which includes the convective term as part of the thermal power into the system, and similarly for

$q_{pc}^*(\mathbf{d}_p)$ when it is excluded;

$$(92) q_{pc}^*(\mathbf{d}_p) = \mathbf{a} IT_{HP} + \mathbf{z}(\mathbf{d}_p) K \Delta T_p - \frac{\mathbf{x}(\mathbf{d}_p)}{2} I^2 R_i$$

The electrical power output is again $I^2 R_i$, so the efficiency

$\mathbf{h}_v(\mathbf{d}_p)$ with the convective term is;

$$(93) \mathbf{h}_v(\mathbf{d}_p) = \frac{W_l}{q_{pv}^*(\mathbf{d}_p)}$$

$$(94) \mathbf{h}_v(\mathbf{d}_p) = \frac{I^2 R_i}{\mathbf{a} IT_{HP} + \mathbf{z}(\mathbf{d}_p) K \Delta T_p - \frac{\mathbf{x}(\mathbf{d}_p)}{2} I^2 R_i + \mathbf{d}_p K \Delta T_p}$$

and without the convective term;

$$(95) \mathbf{h}_c(\mathbf{d}_p) = \frac{W_l}{q_{pc}^*(\mathbf{d}_p)} = \frac{W_l}{\mathbf{a} IT_{HP} + \mathbf{z}(\mathbf{d}_p) K \Delta T_p - \frac{\mathbf{x}(\mathbf{d}_p)}{2} I^2 R_i}$$

$$(96) \mathbf{h}_c(\mathbf{d}_p) = \frac{I^2 R_i}{\mathbf{a} IT_{HP} + \mathbf{z}(\mathbf{d}_p) K \Delta T_p - \frac{\mathbf{x}(\mathbf{d}_p)}{2} I^2 R_i}$$

Both Equations (94) and (96) can be written using Equations (28), (80) and (84) to eliminate I , K and R by introducing the parameters M_p and Z ;

$$(97) \mathbf{h}_v(\mathbf{d}_p) = \frac{\Delta T_p}{T_{HP}} \frac{M_{pv}}{M_{pv} + 1 + \left(\frac{\mathbf{z}(\mathbf{d}_p) + \mathbf{d}_p (M_{pv} + 1)^2}{ZT_{HP}} \right) - \frac{\mathbf{x}(\mathbf{d}_p) \Delta T_p}{T_{HP}}}$$

$$(98) \mathbf{h}_c(\mathbf{d}_p) = \frac{\Delta T_p}{T_{HP}} \frac{M_{pc}}{M_{pc} + 1 + \frac{\mathbf{z}(\mathbf{d}_p) (M_{pc} + 1)^2}{ZT_{HP}} - \frac{\mathbf{x}(\mathbf{d}_p) \Delta T_p}{T_{HP}}}$$

As was done with the conventional case optimizing with respect to M_p yields M_{pv0} and M_{pc0} ;

$$(99) M_{pv0} = \sqrt{1 + Z(\mathbf{z}(\mathbf{d}_p) + \mathbf{d}_p)^{-1} T'_{AVEd}}$$

$$(100) M_{pc0} = \sqrt{1 + Z\mathbf{z}(\mathbf{d}_p)^{-1} T'_{AVEd}}$$

where T'_{AVEd} is defined as;

$$(101) T'_{AVEd} = \left(T_{HH} - \frac{\mathbf{x}(\mathbf{d}_p) \Delta T_p}{2} \right)$$

The optimum efficiencies \mathbf{h}_{v0} and \mathbf{h}_{c0} are found by using Equations (99) and (100) in (97) and (98);

$$(102) \mathbf{h}_{v0} = \frac{\Delta T_p}{T_{HP}} \left(\frac{1}{1 + \frac{2(M_{pv0} + 1)(\mathbf{z}(\mathbf{d}_p) + \mathbf{d}_p)}{ZT_{HP}}} \right)$$

$$(103) \mathbf{h}_{c0} = \frac{\Delta T_p}{T_{HP}} \left(\frac{1}{1 + \frac{2(M_{pc0} + 1)\mathbf{z}(\mathbf{d}_p)}{ZT_{HP}}} \right)$$

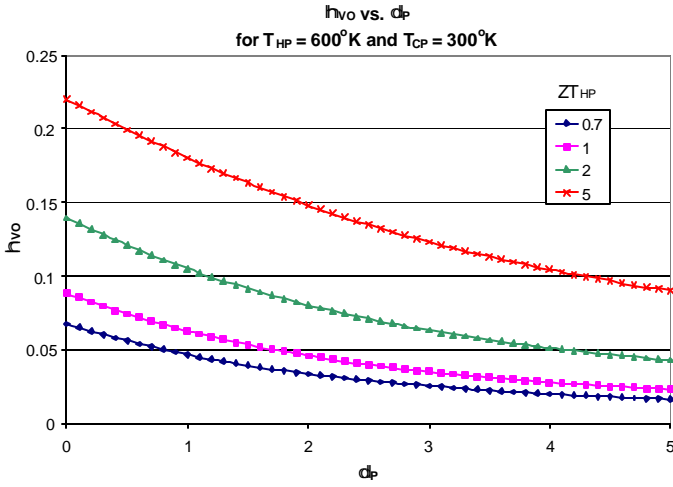


Figure 14.

Figure 14 gives the efficiency h_{v0} as a function of d_p for $T_{HP} = 600^\circ K$, $T_{CP} = 300^\circ K$ and several values of ZT_{HP} . From Figure 14, it is seen that the peak efficiency is at $d_p = 0$, and for small d_p the efficiency slowly decreases. Figure 14 shows the ratio of thermal flux, q_{CP}^* to q_{PV}^* , out the waste (cold) end $T_{CP} = T_p(0)$ as a function of d_p , for the same conditions as Figure 13. Here q_{CP}^* is given by the power into the hot side less the sum of the power into the external load and the convected power out the hot side. It can be expressed in terms of h_{v0} and h_{c0} ;

$$(104) \quad q_{CP}^* = q_P^* (1 - h_{v0}) - d_p K \Delta T_p$$

Or using Equation (95) to eliminate the convective term and expressing the result as a ratio of optimum efficiencies;

$$(105) \quad \frac{q_{CP}^*}{q_{PV}^*} = h_{v0} \left(\frac{1}{h_{c0}} - 1 \right)$$

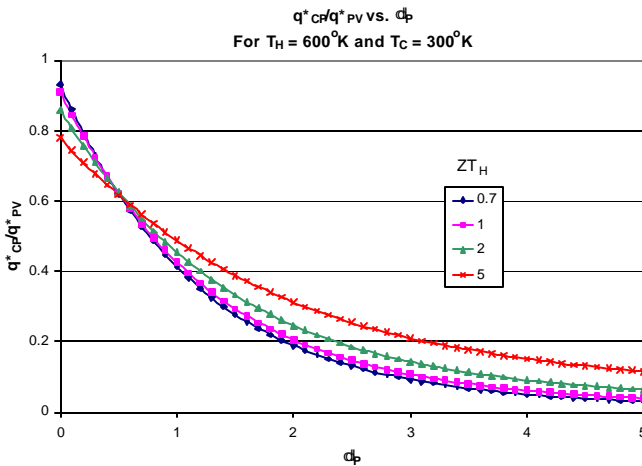


Figure 15.

From Figure 15, it is seen that q_{CP}^* drops rapidly with increasing d_p , so that with modest loss of efficiency

h_{v0} , the waste side heat flux can be reduced substantially, a condition that can be of significant benefit in power generation applications such as power extraction from vehicular exhaust and incineration system waste heat recovery. In such systems, where medium or low quality heat is converted to electrical power, large, expensive or high-power consumption waste heat dissipation at the cold side can strongly affect overall system economic benefit.

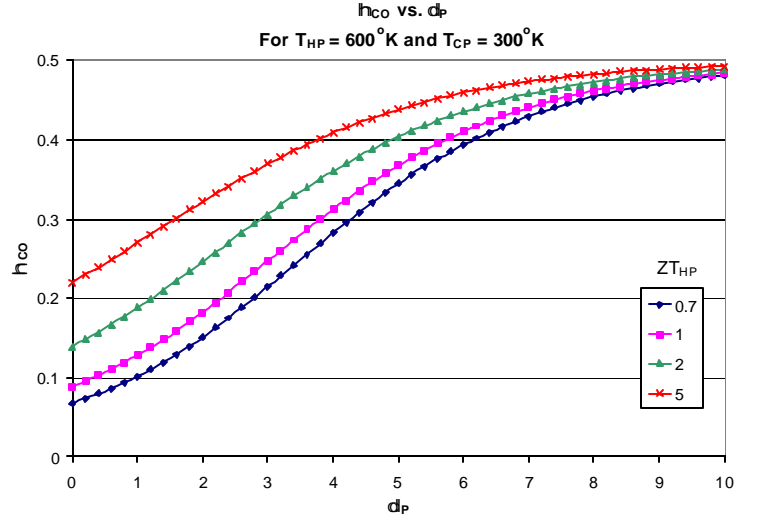


Figure 16.

Figure 16 gives curves for h_{c0} as a function of d_p under the same conditions as for Figure 14. As d_p increases, the efficiency rises rapidly and theoretically approaches Carnot cycle efficiency. To realize the benefits from this configuration, the hot working fluid must be in a form that its thermal power can be of direct use, and not be adversely affected by the constraints placed on it by the TE system. For example, the air or fuel in combustion systems can benefit from preheating and limited amounts of electric power may be produced as a benefit by employing TEs in a preheat system. Steam or air Rankine cycle power generators without regeneration and other co-cycle generators can produce supplemental electric power by adding TE systems that utilize convection to the heating process for their working fluid. Also, mechanical output systems that can benefit from supplemental electrical power generation can use TEs in the preheat process. In these and related systems, the ability of the co-generator to convert efficiently the hot side heat flux from the TE system, determines the net benefit from the combined cycle. The relationship between the cycles can be estimated as follows: Let h_{CG} be the efficiency of the co-generator. Assuming that the combination does not induce or necessitate other important losses, and that the power consumed by pumping fluids through the system can be ignored or are included in cycle efficiencies, system performance can be expressed by the power flow diagram in Figure 17.

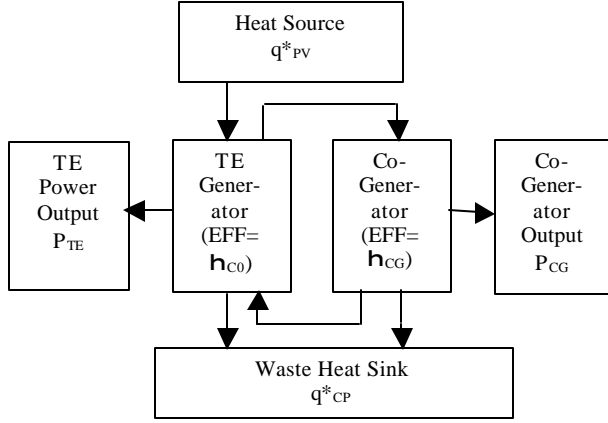


Figure 17.

For this configuration, define $f(\mathbf{d}_p)$ as the ratio of total thermal power to that of the co-generator, \mathbf{h}_{CG} . Let the heat flux to the co-generator be $C_p m \Delta T_p$, then $f(\mathbf{d}_p)$ can be written in terms of q^*_{PV} , the thermal power into the system as;

$$(106) f(\mathbf{d}_p) = \frac{C_p m \Delta T_p}{q^*_{PV}(\mathbf{d}_p)} = \frac{\mathbf{d}_p K \Delta T_p}{q^*_{PV}(\mathbf{d}_p)}$$

The power produced by the TE, P_{TE} is;

$$(107) P_{TE} = \mathbf{h}_{V0} q^*_{PV}(\mathbf{d}_p)$$

The power produced by the co-generator, P_{CG} is;

$$(108) P_{CG} = \mathbf{h}_{CG} C_p m \Delta T_p$$

and from Equation (106);

$$(109) P_{CG} = \mathbf{h}_{CG} q^*_{PV}(\mathbf{d}_p) f(\mathbf{d}_p)$$

The total system efficiency $\mathbf{h}_T(\mathbf{d}_p)$ is found by the sum of P_{TE} and P_{CG} divided by the power in;

$$(110) \mathbf{h}_T(\mathbf{d}_p) = \frac{P_{TE} + P_{CG}}{q^*_{PV}(\mathbf{d}_p)}$$

Using Equations (107) and (109);

$$(111) \mathbf{h}_T(\mathbf{d}_p) = \mathbf{h}_{V0} + f(\mathbf{d}_p) \mathbf{h}_{CG}$$

This is plotted as a function of $f(\mathbf{d}_p)$ in Figure 18 for the same conditions as in Figures 14-16 and several values of ZT_H and \mathbf{h}_{CG} .

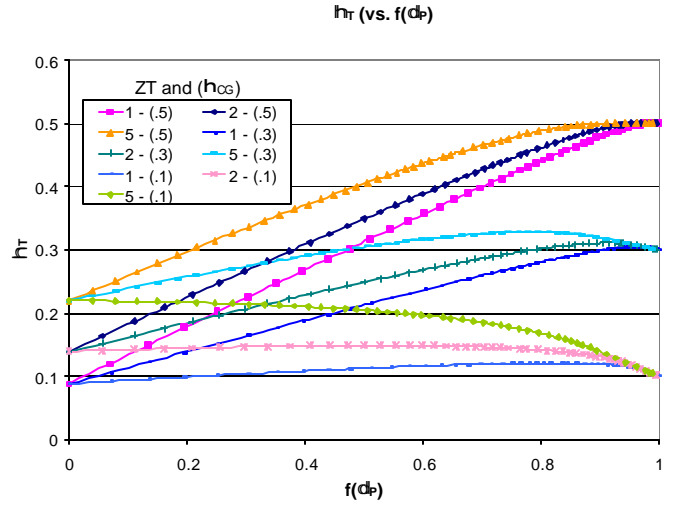


Figure 18.

Figure 18 shows that for $\mathbf{h}_{V0} \approx \mathbf{h}_{CG}$, the system efficiency \mathbf{h}_T is maximized for $f(\mathbf{d}_p)$ between 0 and 1, and not at the limits. Therefore, the combined cycle optimizes efficiency. Further, for $\mathbf{h}_{V0} < \mathbf{h}_{CG}$, there can be a region near $f(\mathbf{d}_p) = 1$ for which \mathbf{h}_T is optimized and a second point at which $\mathbf{h}_T = \mathbf{h}_{CG}$, and for which an amount of electrical power is produced by the convective TE part of the cycle. Thus, the combined cycle can be advantageous to either cycle alone.

Summary and Conclusions

Expressions have been presented for effects of convective flow of media on thermoelectric devices operating in heating, cooling and power generation modes. The equations developed give closed-form solutions for temperature profiles, thermal flux capacity, criteria for optimum performance, and limitations and constraints on performance. The most significant results are Equations (38), (71), (102) and (103) for optimum performance in the several operating modes.

The results show that convection holds the promise of significant performance increase in systems that can utilize a transportable working medium in their function. The working medium can be solid, liquid or gas and can be closed loop (recycling) or make one pass through the system.

Generally, in the cases of cooling and heating, optimum performance is achieved when all of the thermal power appears in the working medium. This requires the capability to use directly and fully the thermal power output contained in the convective media. Thus, the concept is useful for air conditioning, environmental temperature control, industrial flow process control and the like. Refrigeration, semiconductor chip cooler and sensor coolers can derive benefit in the portion of the system that removes waste heat, but the concept is not of value at the heat sink

end (the cold interface) where cooling or some form of temperature control occurs.

Of special significance is the use of convection in power generation. It has been shown that performance is increased in two distinctly different ways. First, waste power out the cold side can be reduced substantially, so that waste side radiators can be smaller, of lower cost and lighter weight. Secondly, when combined in a co-generation cycle that does not utilize exhausted waste heat to preheat incoming working fluid, TE convective power generation can add to capacity, increase efficiency, and provide electrical power output directly from an otherwise mechanical system. Waste power generation appears to be an attractive application area because of the above factors and the potential efficiency gains.

This analysis does not address the impact of loss mechanisms on overall performance that could adversely affect system performance. In the cases of cooling and heating, these mechanisms include temperature differentials between a working medium and the TE element material (if they differ), power dissipated within sintered elements by the passage of viscous working fluids, property changes in the working fluids and the TE materials and performance reduction from parasitic losses over the operating temperature range associated with the construction complexity of such TE elements and systems. Similar losses will exist in power generation systems, although they are likely to have less of an impact since temperature differentials are typically much larger and the TE elements tend to be substantially longer. These issues have to be addressed to successfully achieve the potential benefits from this system.

Further analysis and experiments are the next steps in the evaluation of this power conversion cycle. Studies of solid TE elements that move, and liquid and gaseous working fluids in porous TE systems as well as related designs are being investigated as a continuation of this work.

Acknowledgments

The author is indebted to several colleagues: Mr. R. Diller for simulations and review; Ms. J. Garcia for document preparation; Mr. A. Nannini, numerical simulations and proofreading; and Dr. M. Sussman for helpful discussions and simulations.

References

1. Echigo, R., *et al.*, "An extended Analysis on Thermodynamic Cycle of Advanced Heating/Cooling Method by Porous Thermoelectric Conversion Device", 12th ICT, Yokohama, JAPAN, VI-5 (1993).
2. Tada, S., *et al.*, "A New Concept of Porous Thermoelectric Module Using a Reciprocating Flow for Cooling/Heating System", 15th ICT, Pasadena, U.S.A., 264 (1996).
3. Tada, S., *et al.*, "A New Concept of Porous Thermoelectric Module Using a Reciprocating Flow for

Cooling/Heating System (Numerical Analysis for Heating System)", 16th ICT, Dresden, GERMANY (1997).

4. Angrist, S., Direct Energy Conversion, Third Edition, Allyn and Bacon, Inc. (Boston, 1976), Chapter 4, pp. 140-165.